Resonance Raman Spectral Properties and Stability of Manganese Protoporphyrin IX Cytochrome b_5[†]

Larry D. Gruenke,[‡] Jie Sun,[§] Thomas M. Loehr,[§] and Lucy Waskell*[,‡]

Department of Anesthesia and the Liver Center, University of California, San Francisco, and the Department of Anesthesia, Veterans Administration Medical Center, San Francisco, California 94121, and Department of Chemistry, Biochemistry, and Molecular Biology, Oregon Graduate Institute of Science and Technology, Portland, Oregon 97291-1000

Received February 21, 1997[⊗]

ABSTRACT: The structure and stability of cytochrome b_5 reconstituted with manganese protoporphyrin IX instead of iron protoporphyrin IX has been investigated by resonance Raman spectroscopy and stopped-flow visible spectroscopy. The resonance Raman spectrum of Mn^{III} cytochrome b_5 was consistent with a high-spin hexacoordinate Mn^{III} protoporphyrin IX structure that converted to a high-spin pentacoordinate structure at higher laser power. The resonance Raman spectrum of Mn^{II} cytochrome b_5 indicated a high-spin pentacoordinate structure which was independent of laser power. Studies of the binding of Mn^{III} protoporphyrin IX to apocytochrome b_5 indicated that the Mn^{III}-containing porphyrin bound much less tightly to the protein than did heme. Although the second-order rate constant at 20 °C for the association of heme with apocytochrome b_5 (4.5×10^7 M^{-1} s^{-1}) was estimated to be only 1 order of magnitude higher than that with Mn protoporphyrin IX (3.3×10^6 M^{-1} s^{-1}), the dissociation of manganese substituted cytochrome b_5 into the apoprotein and free Mn protoporphyrin IX occurs with a first-order rate constant of 1.2×10^{-2} s^{-1} at 20 °C while the dissociation of heme from cytochrome b_5 at room temperature occurs 3 orders of magnitude more slowly with a first-order rate constant of 1.67×10^{-5} s^{-1} [Vergeres, G., Chen, D. Y., Wu, F.F., & Waskell, L. (1993) *Arch. Biochem. Biophys. 305*, 231−241]. The equilibrium dissociation constant for manganese-substituted cytochrome b_5 increased with temperature from 4 nM at 20 °C to 14 nM at 37 °C. These results suggest that, in the reconstituted cytochrome P450 metabolizing system, especially in studies done with low protein concentrations (0.1 μM), and at elevated temperatures (37 °C), as much as 30% of the manganese-substituted cytochrome b_5 may dissociate to free Mn−protoporphyrin IX and apocytochrome b_5.

Cytochrome b_5 increases the efficiency of catalysis in the purified reconstituted cytochrome P450 metabolizing system from mammalian hepatic endoplasmic reticulum; that is, more of the NADPH that is consumed is utilized to produce product rather than oxidative side products when cytochrome b_5 is present. With most substrates, the presence of cytochrome b_5 has only a modest influence on the rate of product formation, and in the instances where it has been studied the improved efficiency of ≅15−20% is a result of decreased production of oxygenated side products, particularly the superoxide radical anion. In contrast, with a minority of substrates such as methoxyflurane, nifedipine, *p*-nitroanisole, prostaglandin, lauric acid, methylcarbazole, chlorobenzene, *p*-nitrophenetole, 7-ethoxycoumarin, benzo[*a*]pyrene, lidocaine, and testosterone β-hydroxylation, product formation is greatly stimulated when cytochrome b_5 is present. Why the influence of cytochrome b_5 should be so different for these two classes of substrates has been a long-standing question (Gruenke et al., 1995). Mechanistic studies suggest that the effect of cytochrome b_5 on the cytochrome P450 reconstituted system occurs at multiple steps in the reaction cycle and that more than one mechanism is involved. In an effort to separate which effects of cytochrome b_5 on the cytochrome P450 system are a result of the ability of cytochrome b_5 to provide the second electron in the cytochrome P450 reaction cycle, and which are due to possible allosteric effects, we and others (Canova-Davis et al., 1985; Cinti & Ozols, 1975; Morgan & Coon, 1984; Tamburini & Schenkman, 1987) have examined cytochrome P450 catalyzed metabolism in the presence of Mn cytochrome b_5. Under aerobic conditions, Mn cytochrome b_5 exists as Mn^{III} cytochrome b_5. It has been assumed to have essentially the same structure as ferric cytochrome b_5 but functionally differs from native cytochrome b_5 because it is not capable of donating electrons to cytochrome P450 (Morgan & Coon, 1984). The use of manganese analogs of heme proteins has been successfully used in studies of myoglobin and hemoglobin, among others, and in the case of hemoglobin, a crystal structure has been obtained which confirms that the substitution with manganese protoporphyrin IX (Mn PPIX)[1] has resulted in minimal structural changes in the protein itself (Moffat et al., 1976).

Our intention in the present work was to more closely examine the structure and stability of Mn cytochrome b_5 in order to further evaluate our previous assumption that the structure of Mn cytochrome b_5 and native cytochrome b_5

[†] Supported by National Institutes of Health Grants GM 35533 (L.W.) and GM34468 (T.M.L.) and by a Veterans Administration Merit Review (L.W.).

* Correspondence should be addressed to this author at Veterans Administration Medical Center Department of Anesthesia (129), 4150 Clement Street, San Francisco, CA 94121.

[‡] UCSF and VA Medical Center.

[§] Oregon Graduate Institute of Science and Technology.

[⊗] Abstract published in *Advance ACS Abstracts,* May 15, 1997.

[1] Abbreviations: DME, dimethyl ester; Im, imidazole; Mn cytochrome b_5, cytochrome b_5 reconstituted with manganese protoporphyrin IX; PPIX, protoporphyrin IX; Py, pyridine; TPP, tetraphenylporphyrin.

S0006-2960(97)00407-8 CCC: $14.00

were similar enough to be considered functionally identical in the reconstituted cytochrome P450 system. The structure of trypsin-solubilized Mn cytochrome b_5 was probed by its resonance Raman spectral characteristics. Mn^{III} cytochrome b_5, which is the form that exists in the presence of oxygen, was found to be hexacoordinate and therefore is presumed to be very similar in structure to both ferrous and ferric cytochrome b_5 except for a $Mn^{III}-N_\epsilon$ histidine bond length of ~2.3 Å (W. R. Scheidt, personal communication) versus an iron N_ϵ histidine bond length of 2.04 Å (Argos & Mathews, 1975). However, the experimentally determined K_d for the equilibrium between Mn cytochrome b_5 and apocytochrome b_5 + Mn PPIX under the usual conditions of the reconstituted cytochrome P450 system indicates that up to one-third of the cytochrome b_5 may be present as apocytochrome b_5 which clearly has a different structure than the heme containing cytochrome b_5 (Falzone et al., 1996).

MATERIALS AND METHODS

Chemicals. Hemin was obtained from Sigma (St. Louis, MO, cat. no. H2250). Manganese protoporphyrin IX was obtained from Porphyrin Products (Logan, UT). Other chemicals used were reagent grade. Stock solutions of heme (0.1 mg/mL) were made by adding hemin to 50% ethanol followed by careful dropwise addition with stirring of 1 M sodium hydroxide until all of the hemin dissolved. Stock solutions of Mn PPIX were prepared in a similar manner.

Preparation and Characterization of Soluble Apocytochrome b_5 and Mn Cytochrome b_5. Bovine cytochrome b_5 was isolated from hepatic microsomes following their treatment with trypsin as described by Reid and Mauk (1982). The product obtained gave a single band on SDS polyacrylamide gels and an A_{412}/A_{280} ratio of 5.9. Soluble apocytochrome b_5 was obtained by treatment of soluble bovine cytochrome b_5 with 0.2% HCl in acetone as described by Cinti and Ozols (1975), except that deoxycholate was omitted from the buffers and the precipitated protein was washed with an additional aliquot of acetone-HCl to remove any remaining traces of heme. A UV/vis spectrum of the apoprotein showed that less than 0.5% of the original heme remained. Concentrations of heme were determined spectrophotometrically using an extinction coefficient of $\epsilon_{385} = 56\ mM^{-1}\ cm^{-1}$ (Ozols & Strittmatter, 1964) in 100 mM pH 7.9 Tris buffer. The concentration of apocytochrome b_5 solutions was estimated from the amount of cytochrome b_5 produced on titration with heme as described by Rogers and Strittmatter (1974). Concentrations of Mn PPIX were determined by weight. A titration of the apocytochrome b_5 solution with Mn PPIX confirmed the expected 1:1 stoichiometry.

Soluble Mn cytochrome b_5 was prepared by adding a 1.5-fold molar excess of Mn PPIX to apocytochrome b_5 followed by chromatography on a Sephadex G-25 column (Cinti & Ozols, 1975). It was estimated from non-denaturing polyacrylamide gels that Sephadex-treated Mn cytochrome b_5 contained about 25% apoprotein. The product was therefore treated a second time with an amount of Mn PPIX in 50% ethanol slightly in excess of the amount of the apoprotein estimated to be present. After incubation for 1 h at room temperature the mixture was filtered through a 0.2 μ filter and concentrated, diluted in 20 mM Tris-HCl (pH 8.1) and then reconcentrated to 50 mg/mL using a 3 kDa Centricon filter. This product, designated here as Mn cytochrome b_5 Batch I, gave a single band on both denaturing and non-denaturing polyacrylamide gels, but titration with heme (see below) revealed that this batch contains about 20% of apocytochrome b_5. An aliquot of this material was treated for a third time with Mn PPIX (0.15 equiv/equiv protein present) and was reconcentrated as above. The product from this extra treatment with Mn PPIX is designated here as Mn cytochrome b_5 Batch II and was assumed to consist only of holoprotein, because it did not reveal the presence of apocytochrome b_5 when it was titrated with heme.

Determination of the Equilibrium Dissociation Constant of Mn PPIX Dimer. It has been known for many years that hemes and other metalloporphyrins aggregate in aqueous solutions (White, W., 1978). Aggregation of a compound is assumed to occur if the Beer−Lambert law is not obeyed. Moreover, the observation of a well-defined isosbestic point suggests the presence of two species only. Since Mn^{III} protoporphyrin IX, under the conditions of our experiment, did not obey the Beer−Lambert law and exhibited a well-defined isosbestic point, it was assumed that dimerization was occurring. In order to relate the spectral changes which occurred with dimerization to the concentration of the monomer, we followed the experimental approach of Brown et al. (1970). The absorbance of a Mn PPIX solution at 464 nm is related to the concentration of the monomer and dimer in solution as described in the equation

$$A_{464} = \epsilon_d[D] + \epsilon_m[M]$$

where A_{464} is the absorbance at 464 nm in the experimental spectrum, ϵ_d is the extinction coefficient of the dimer at 464 nm, [D] is the dimer concentration, ϵ_m is the extinction coefficient of the monomer at 464 nm, and [M] is the monomer concentration.

In order to make the spectral changes at different concentrations more comparable, the spectra were normalized by dividing by the total concentration (T) of Mn PPIX present in solution.

$$A_{464}/T = \epsilon_d[D]/T + \epsilon_m[M]/T \quad (1)$$

Since

$$[D] = (T - [M])/2 \quad (2)$$

$$A_{464}/T = \epsilon_d(T - [M])/2T + \epsilon_m[M]/T \quad (3)$$

Simplifying,

$$A_{464}/T = \epsilon_d/2 + (\epsilon_m - \epsilon_d/2)[M]/T \quad (4)$$

Constants can be combined to define new parameters:

$$E_o = \epsilon_d/2 \quad (5)$$

$$E_c = (\epsilon_m - \epsilon_d/2) \quad (6)$$

Thus eq 4 becomes

$$A_{464}/T = E_o + E_c[M]/T \quad (7)$$

The dissociation of the presumed Mn PPIX dimer is independent of pH and occurs according to the following

reaction:

$$\text{dimer} \leftrightarrow \text{monomer} + \text{monomer} \quad (8)$$

The equilibrium dissociation constant is given by the equation

$$K_d = [M]^2/[D] \quad (9)$$

Substituting for [D] from eq 2 above:

$$K_d = 2\,[M]^2/(T - [M]) \quad (10)$$

or

$$[M]^2 + [M]K_d/2 = K_dT/2 \quad (11)$$

Completing the square,

$$([M] + K_d/4)^2 = K_dT/2 + K_d^2/16 \quad (12)$$

Taking the square root and solving for [M],

$$[M] = \sqrt{K_dT/2 + K_d^2/16} - K_d/4 \quad (13)$$

Inserting this into eq 7,

$$A_{464}/T = E_o + E_c/T\,(\sqrt{K_dT/2 + K_d^2/16} - K_d/4) \quad (14)$$

The UV/vis spectra (300−650 nm) of Mn PPIX in 50 mM potassium phosphate buffer at pH 7.4 were recorded at concentrations ranging from 0.2−20 μM. The experimentally measured absorbance of the Mn PPIX solutions were fit to equation 14 by nonlinear regression to determine the parameters E_o, E_c, and K_d. Absorbance was measured at 20, 30, 35, and 45 °C at pH 7.4. The spectra were also recorded at 30 °C at a pH of 7.0, 7.4, 8.0, and 9.0.

The rate constant for the dissociation of Mn PPIX dimer into its monomer was determined using a Hi-Tech SF-40 stopped-flow spectrophotometer (Salisbury, U.K.) interfaced to an IBM compatible computer. The sample cell of the stopped-flow spectrometer has a 1 cm light path and is immersed in a temperature-controlled bath. Mathematical analysis of the kinetic data was accomplished by nonlinear regression fitting using the program provided by Hi-Tech. Complete spectra between 320 and 620 nm were obtained on the same instrument with the rapid scan monochromator module. Spectral changes upon dilution of Mn PPIX were followed at 30 °C and at 464 nm in fixed wavelength experiments. One syringe contained 4.0 μM Mn PPIX in a 50 mM potassium phosphate buffer, pH 7.4, and the other syringe contained buffer alone.

The rate constant for the reaction of Mn PPIX with heme was obtained in a similar manner with 4.0 μM Mn PPIX in a 200 mM potassium phosphate buffer, pH 7.35, in one syringe and 4.4 μM heme in 0.1 mM sodium hydroxide in the other syringe. The final pH of the solution after mixing was 7.4.

Difference Spectra. For each of the reactions studied, the UV/vis spectra of individual reactants and products were obtained using a Cary 1 spectrophotometer. Difference spectra for the reaction of apocytochrome b_5 with heme or Mn PPIX were obtained by subtracting the normalized heme (1.81 μM at pH 7.9) or Mn PPIX spectrum (3.84 μM, pH 7.4) from the spectrum of cytochrome b_5 or of Mn cytochrome b_5, respectively. For the reaction of Mn cytochrome b_5 with heme, the difference spectrum, (cytochrome b_5 plus Mn PPIX) minus (Mn cytochrome b_5 plus heme), was calculated from the individual spectra. Difference spectra were obtained experimentally in a split cell with a 0.9 cm path length divided into two equal compartments. Mn cytochrome b_5 (1.76 nmol) dissolved in 1.00 mL of 100 mM pH 7.35 potassium phosphate buffer, was placed in one compartment of the split cell and 2.72 nmol of heme in 1.00 mL of the same buffer were placed in the other compartment of the split cell. The spectrum was recorded as a base line and then the contents of the split cell were mixed by repeated inversions of the cell. After 20 min at 30 °C, the difference in the spectrum was recorded. Absorbance readings were corrected for path length. Difference spectra were obtained in a similar manner using apocytochrome b_5 with an excess of heme and apocytochrome b_5 with an excess of Mn PPIX.

Resonance Raman Spectra. A solution of Batch I Mn^{III} cytochrome b_5 (10 μL of a 367 μM solution) was placed in a glass capillary tube for UV/vis and resonance Raman measurements (Loehr & Sanders-Loehr, 1993). The spectrum of the oxidized protein contains peaks characteristic for Mn^{III} PPIX at 469, 556, and 589 nm. Mn^{II} cytochrome b_5 was prepared by flushing a 10 μL sample of 367 μM Mn^{III} cytochrome b_5 with argon in a septum-sealed Pasteur pipette and then adding 10 μL of a freshly prepared solution of 20 mM sodium dithionite. Complete reduction took about 10 min as judged by the emergence of a new Soret absorption peak at 433 nm and the complete disappearance of the 469 nm peak. The resonance Raman spectra of Mn^{III} cytochrome b_5 and Mn^{II} cytochrome b_5 were obtained on a DILOR Z-24 spectrophotometer with 476.5-nm (Ar^+ laser) and 413.1-nm (Kr^+ laser) excitation, respectively, in a 90°-scattering geometry with the sample cooled to ∼5 °C. Spectral resolution was ∼5 cm^{-1}. Signal-to-noise was improved by two to three repetitive scans acquired at a rate of 1 cm^{-1} s^{-1}. Sample integrity was monitored by UV/vis spectroscopy before and after each resonance Raman experiment.

Determination of the Rate Constants for the Association of Apocytochrome b_5 with Heme and Mn PPIX. The reaction of apocytochrome b_5 with heme or Mn PPIX was followed spectrophotometrically in a Hi-Tech SF-40 stopped-flow spectrophotometer.

During the association reactions, complete spectra were recorded every 100 ms for 4.8 s at 10 °C. The concentration of apocytochrome b_5 was either 2 or 4 μM in one syringe and an equivalent concentration of heme or Mn PPIX was in the second syringe.

Association reactions were also examined in the stopped-flow spectrophotometer at fixed wavelength under pseudo-first-order conditions with at least a 5-fold excess of heme. One driving syringe contained the apoprotein in 100 mM potassium phosphate buffer (pH 7.35), and the second syringe contained heme (or Mn PPIX) in 0.4 mM sodium hydroxide. (Heme solutions are more stable in alkaline solutions.) The pH of these solutions after mixing was 7.41. The association of apocytochrome b_5 with heme was followed at 414 nm with an apocytochrome b_5 concentration of 0.1 μM and a heme concentration which varied from 0.5 to 2.0 μM. The association of apocytochrome b_5 with Mn PPIX was followed at 470 nm with apocytochrome b_5 concentrations between 0.14 and 0.35 μM and the appropriate 5-fold or greater

concentration of Mn PPIX. For each experiment 500 data points were collected at fixed time intervals.

Characterization of Mn Cytochrome b_5 Solutions. Because of the relatively loose binding of Mn PPIX to apocytochrome b_5 compared to heme, it was necessary to determine the amount of apocytochrome b_5 in the concentrated stock solution ($\cong$170 μM) of Mn cytochrome b_5 Batch I and II. It is possible to distinguish between apocytochrome b_5 and Mn cytochrome b_5 in a mixture because the reaction of apocytochrome b_5 with heme results in a marked increase in absorbance at 414 nm but only minimal changes at 470 nm. The dissociation of Mn PPIX from Mn cytochrome b_5, however, results in a marked decrease in absorbance at 470 nm but only minimal change at 414 nm. To determine the relative amounts of apo and holo protein, the concentrated solution must be diluted. Because of the large K_d of Mn cytochrome b_5 which had been independently determined, significant dissociation of Mn PPIX from Mn cytochrome b_5 occurred upon dilution. Thus, the diluted solution to be measured contained apocytochrome from two sources: (1) the original concentrated solution and (2) that which dissociated from Mn cytochrome b_5 as a result of dilution. The amount of apocytochrome b_5 in the original concentrated solution was calculated by measuring the total amount of apocytochrome b_5 in the diluted solution and subtracting the amount calculated to have been generated upon dilution by dissociation of Mn cytochrome b_5. The K_d of Mn cytochrome b_5 used in this calculation was measured in independent experiments under identical conditions (K_d = 7 nM at 30 °C).

The concentrations of apocytochrome b_5 and Mn cytochrome b_5 in the Batch I and II Mn cytochrome b_5 preparations were determined by adding a 20 μL aliquot of the Batch I or Batch II stock solutions, which were estimated to be about 170 μM, to a 1-mL cuvette containing 0.98 mL of pH 7.35 potassium phosphate buffer. This cuvette was placed in the sample beam of the spectrophotometer, and a cuvette containing 1.00 mL of buffer alone was placed in the reference beam. Aliquots of a 55.7 μM solution of heme in a 1:1 mixture of ethanol and 0.4 mM sodium hydroxide were added to the sample and reference cuvettes at 30 °C and absorbance changes were followed at 470 nm relative to those at 490 nm where there are no absorbance changes during this complex reaction. Final absorbance was corrected for dilution which was 15% or less of the initial volume. Plots of these absorbance changes vs the amount of heme added were analyzed as follows: The first titration end point was determined by extrapolation of the linear portion of the titration curve back to the *x*-axis (zero absorbance change), while the second end point was indicated by a change in the slope of the absorbance data. The total amount of apocytochrome b_5 present was calculated from the amount of heme added at the first end point. This was considered to be the total amount of apocytochrome b_5 present in the diluted solution and was used to calculate the amount of apocytochrome b_5 present in the stock solution as described in the previous paragraph. This procedure and analysis was validated by adding heme to a solution with a known amount of Mn cytochrome b_5 and apocytochrome b_5 which had been generated by incrementally adding Mn PPIX to an apocytochrome b_5 solution.

Determination of the Rate Constant of the Dissociation of Mn Cytochrome b_5 into Apocytochrome b_5 and Mn PPIX. Preliminary studies had indicated that the association of heme and apocytochrome b_5 was essentially irreversible, and the rate constant was $\cong$100-fold faster than the dissociation of Mn PPIX from Mn cytochrome b_5. The ligand displacement method was therefore used to determine the rate constant for dissociation of Mn cytochrome b_5 into its two components, apocytochrome b_5 and Mn PPIX. Briefly, this involved rapidly mixing a solution of Mn cytochrome b_5 with an excess of heme and following the reaction in the stopped-flow spectrophotometer at the appropriate wavelengths.

(A) Rapid Scan Studies. During the reaction of Mn cytochrome b_5 with heme a total of 48 spectra between 320 and 620 nm were obtained over a period of 96 s at 25 °C. One driving syringe contained a 3 μM solution of Mn cytochrome b_5 in 100 mM pH 7.35 potassium phosphate buffer and the second syringe contained a 3 μM solution of heme in 0.4 mM sodium hydroxide.

(B) Fixed Wavelength Studies. The dissociation of Mn cytochrome b_5 into apocytochrome b_5 and Mn PPIX was followed in the stopped-flow spectrophotometer at 414 nm, the wavelength at which the formation of cytochrome b_5 is observed. Mn cytochrome b_5 (0.6−1.0 μM) in 100 mM pH 7.35 potassium phosphate buffer was placed in one driving syringe, and at least a 3-fold excess of heme in 0.4 mM sodium hydroxide was placed in the second syringe. Because the initial absorbance data indicated two kinetic phases with nearly a 100-fold difference in rates, the experiments were repeated. This time, however, 750 absorbance data points were collected at increasing time intervals (logarithmically) so that there would be a sufficient number of data points in each of the phases. The pH dependence of the rate constants for the dissociation reaction was examined using Batch I Mn cytochrome b_5 in 100 mM 1:1 phosphate−borate buffers. The pH values given are those measured in the final reaction solution after mixing with an equal volume of 0.4 mM sodium hydroxide.

RESULTS

Resonance Raman Spectroscopy. Since the chemical properties of metalloporphyrins have been rigorously correlated with the frequency positions of certain characteristic resonance Raman spectral features (Mino et al., 1988; Spiro, 1983), resonance Raman spectroscopy is a powerful probe of the structural properties of active site hemes. The high-frequency region (1300−1700 cm^{-1}) is most revealing about the oxidation state of the metal (from ν_4, the pyrrole C−N vibration) and its spin and coordination states (from ν_2, ν_3, ν_{10}, and ν_{19}). All of these frequencies correspond to skeletal vibrations of the porphyrin macrocycle. The low-frequency region (200−800 cm^{-1}) is most informative for the identification of axial ligands of the metal in the porphyrin (Spiro, 1983; Yu, 1986).

Thus, ν_4 corroborates the oxidation state (generally known from the UV/vis spectrum) and monitors any changes that may be chemically induced or photoinduced. In heme proteins the Fe−N_{his} frequency inversely correlates with the porphyrin vibration, ν_4 (Stavrov, 1993). The frequencies ν_3, ν_{10}, and ν_{19} reflect the spin state, and their positions are further subdivided among penta- and hexacoordinate states. Frequencies for a variety of metal-substituted hemes and metal octaethylporphyrin model systems (metal = Mn, Co, Ni, Cu) have been studied (Parthasarathi & Spiro, 1987;

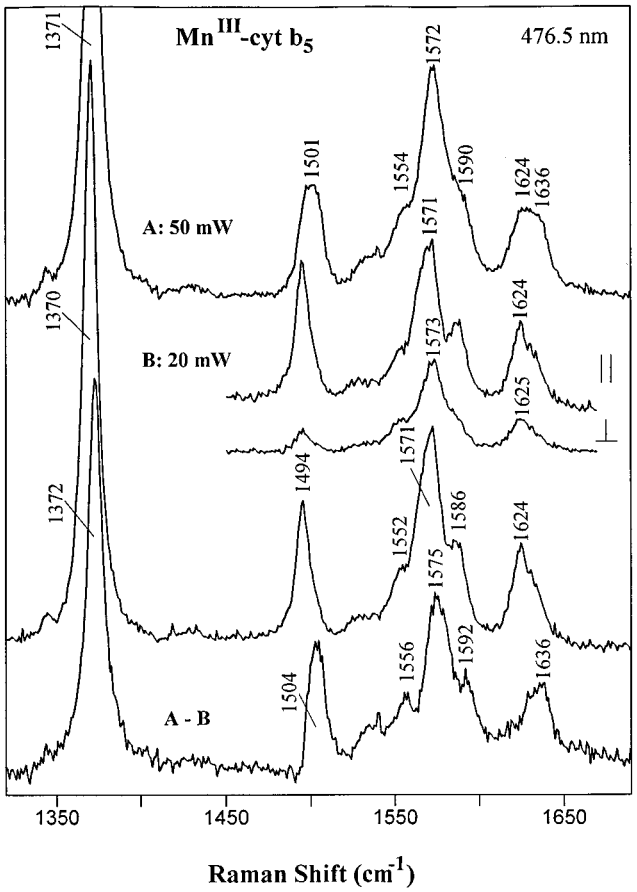

FIGURE 1: Resonance Raman spectra of oxidized Mn^{III} cytochrome b_5 as a function of laser power with 476.5-nm excitation. (A) With 50 mW, the spectrum is that of a five- and six-coordinate mixture. (B) With 20 mW, the spectrum is largely that of the six-coordinate species. The parallel (||) and perpendicular (⊥) polarization data (1450−1650 cm^{-1}) are shown above the scrambled polarization spectrum. The bottom trace, A − B, is the difference spectrum and represents largely the pure five-coordinate species.

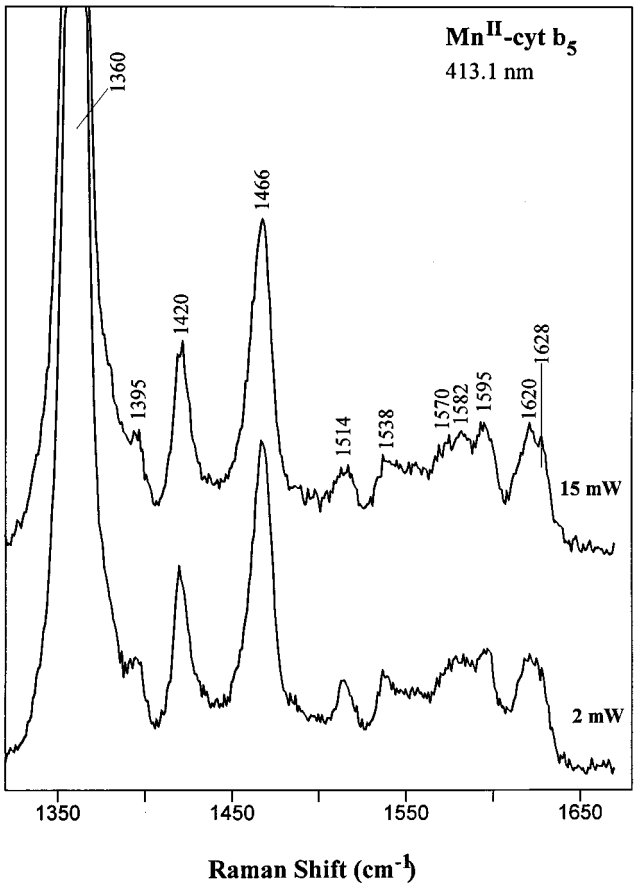

FIGURE 2: High-frequency resonance Raman spectra of Mn^{II} cytochrome b_5 as a function of laser power (2 and 15 mW) with 413.1-nm excitation.

Oertling et al., 1987); the following table highlights some of the data available for Mn systems:

Mn PPIX	ν_4	ν_3	ν_{19}	ν_{10}
III HS 5	~1370	~1500	~1580	~1634
III HS 6	~1369	~1494	~1574	~1627
II HS 5	~1357	~1464	~1540	~1593

In the table, the roman numeral indicates the oxidation state, HS refers to high-spin, and 5 and 6 indicate pentacoordinate and hexacoordinate, respectively.

The resonance Raman spectrum of Mn^{III} cytochrome b_5 is shown in Figure 1. This spectrum is dependent on the laser power and, thus, indicative of a photoinducible structural change. At low power (~20 mW), the spectrum is characteristic of a six-coordinate, high spin Mn^{III} PPIX (Figure 1B). The polarized band at 1494 cm^{-1} can be assigned as the porphyrin mode ν_3. The band at 1571 cm^{-1} is also polarized and assigned to ν_2; in perpendicular polarization an inversely polarized band appears at 1573 cm^{-1} that is assigned to ν_{19}. The band at 1624 cm^{-1} is a mixture of a vinyl stretching vibration (polarized) and porphyrin skeletal mode ν_{10} (depolarized) as judged from the polarization analysis. In perpendicular polarization, the intensity of this band is mainly from ν_{10} at 1625 cm^{-1}. These values are comparable with ν_3, ν_2, and ν_{10} of [(Py) $_2$Mn^{III}-PPIXDME] reported at 1494, 1573, and 1626 cm^{-1}, respectively (Parthasarathi & Spiro, 1987), and provide evidence that Mn^{III} cytochrome b_5 is a six-coordinate high spin species with the Mn^{III} in the plane of the heme. The axial ligands are most likely the two histidines coordinated to the heme of native cytochrome b_5 (Argos & Mathews, 1975), however, a His/Aqua ligation set cannot be ruled out.

Upon raising the power to 50 mW, some changes occur in the resonance Raman spectrum. The ν_3 and ν_{10} bands broaden, and new features grow in at 1504 and 1636 cm^{-1}, respectively. These higher frequency components are indicative of a switch from predominantly six- to five-coordinate Mn^{III}PPIX. The difference spectrum in the bottom of Figure 1 shows the peaks associated with a pure five-coordinate species. For comparison, the ν_3 and ν_{10} Raman bands have been reported at 1500 and 1634 cm^{-1}, respectively, for the authentic pentacoordinate (Ac)Mn^{III}-PPIXDME (Parthasarathi & Spiro, 1987). The formation of the five-coordinate Mn^{+3} cytochrome b_5 implies that one of the axial ligands photodissociates under higher laser power.

The resonance Raman spectrum of Mn^{II} cytochrome b_5, which was obtained under anaerobic conditions with higher energy 413-nm excitation is independent of the laser power (Figure 2). The frequencies of almost all the Raman bands are similar (within 3 cm^{-1}) to those of the high-spin, pentacoordinate (2-MeIm)Mn^{II}PPIX (Parthasarathi & Spiro, 1987). The reduced metal is indicated by the lower frequency of ν_4 at 1360 cm^{-1} vs 1370 cm^{-1} for the oxidized form. Two exceptions are a weak, overlapped band at 1582 cm^{-1} and another at ~1630 cm^{-1}. The former may cor-

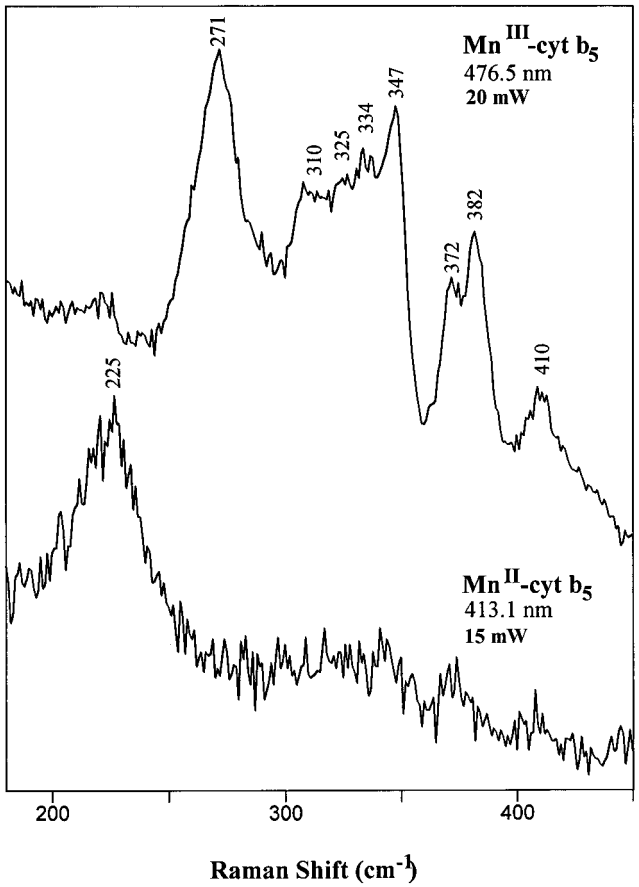

FIGURE 3: Low-frequency resonance Raman spectra of Mn^{III} and Mn^{II} cytochrome b_5. The band at 225 cm^{-1} in the reduced form of the protein is assigned to ν[Mn^{II}−N(histidine)].

respond to the 1575 cm^{-1} band of (2-MeIm)Mn^{II}PPIX that has been assigned as ν_{37}. The *depolarized* band at 1630 cm^{-1} has no counterpart in the (2-MeIm)Mn^{II}PPIX spectrum. Although we cannot unambiguously assign this band at present, it may be a second vinyl stretching frequency since there are two vinyl groups, or it may arise from a different vinyl orientation (Kalsbeck et al., 1995). The vinyl mode at ~1620 cm^{-1} is always intense and polarized with Soret excitation. The Raman bands at 1467 cm^{-1} (ν_3, polarized) and 1595 cm^{-1} (ν_{10}, depolarized) for Mn^{II} cytochrome b_5 indicate that its manganoporphyrin is five-coordinate.

The axial ligand, of course, is expected to be a histidine. The low-frequency region of the Mn^{II} cytochrome b_5 resonance Raman spectrum is dominated by a single band at 225 cm^{-1} (Figure 3) and suggests a five-coordinate histidine-bound Mn^{II} PPIX. In other manganoporphyrins, a Mn−N(Im) stretching band at 215 cm^{-1} usually dominates the resonance Raman spectrum: examples include (Im)Mn^{II} PPIX (220 cm^{-1}), Mn^{II} myoglobin (215 cm^{-1}), Mn^{II} hemoglobin (216 cm^{-1}), and the Mn^{II} PPIX−heme oxygenase complex (212 cm^{-1}) (Sun et al., 1993). The higher frequency of the Mn^{II} cytochrome b_5 reflects a stronger Mn−histidine bond with a shorter bond length or, alternatively, with significant hydrogen bonding of the non-coordinated imidazole nitrogen atom of this proximal ligand. The correlation of the Fe−N(His) vibrational frequency with the strength of hydrogen bonding of the proximal histidine has been well documented for hemoglobin, myoglobin, and peroxidases (Smulevich et al., 1988; Stavrov, 1993; Teraoka & Kitagawa, 1981). For symmetrical Mn^{III} porphyrins with two histidine

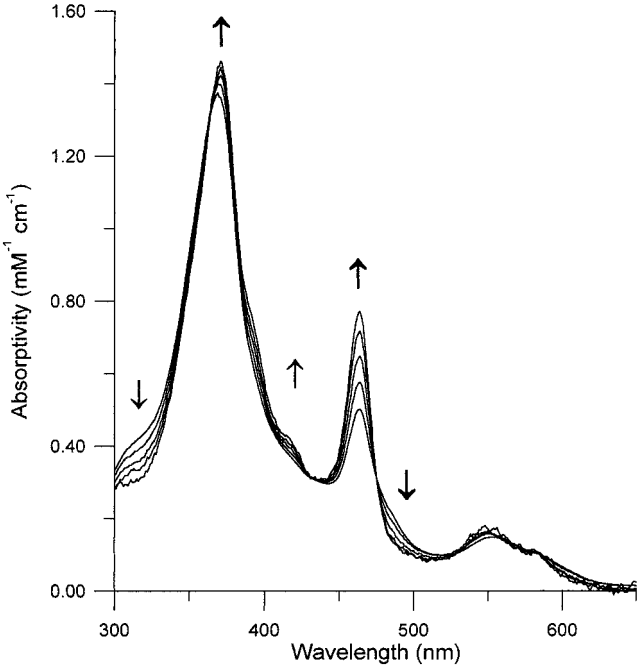

FIGURE 4: Normalized UV/vis absorption spectra of Mn PPIX at concentrations of 0.5, 1.0, 2.0, 5.0, and 20 μM. The arrows indicate the direction of change with dilution.

or imidazoles, the metal−histidine vibrations are generally not observed. In agreement with this expectation, the Mn^{III} axial vibrations were not observed in the Mn^{III} cytochrome b_5 spectrum (Figure 3, top). Here, many of the dominant bands are porphyrin out-of-plane deformation modes.

Determination of the Fe and Mn PPIX Monomer Concentration Using the Experimentally Calculated Equilibrium Constants. Under our experimental conditions it could be shown that the Beer−Lambert law was not obeyed by solutions of Fe and Mn PPIX and that the concentration dependent spectral changes exhibited an isosbestic point. This indicated that aggregation, most likely dimerization, of the metalloporphyrins was occurring at the porphyrin concentrations used in our experiments. Furthermore, it was assumed that only the metalloporphyrin monomer was able to react with apocytochrome b_5. Thus, it was essential to know the monomer concentration present in solution during the association reaction between the apoprotein and metalloporphyrins. Brown et al. (1970) demonstrated that Fe^{III} PPIX dimerized according to the following reaction with an equilibrium association constant of 4.5.

$$\text{monomer} + \text{monomer} \rightarrow \text{dimer} + H^+$$

The dimerization of heme under the experimental conditions used in these studies results in the formation of a μ oxo-dimer (Brown, et al. 1969).

Since similar information was not available in the literature for Mn^{III} PPIX, the equilibrium dissociation constant of the presumed Mn^{III} PPIX dimer was determined experimentally for the following reaction using a method similar to that used by Brown et al. (1970):

$$\text{dimer} \leftrightarrow 2\ \text{monomer}$$

The normalized spectral changes which occur upon dilution of Mn^{III} PPIX at pH 7.4 and 30 °C are shown in Figure 4. Note the well-defined isosbestic point at 475 nm. These

changes are similar over the pH range 7−9 in contrast to those of Fe^{III} PPIX solutions where the spectral changes on dilution are pH dependent. The lack of pH dependence of the Mn^{III} PPIX dimerization (between pH 7 and 9) suggests that this process may not result in the formation of a μ-oxo dimer as occurs with heme (Loach & Calvin, 1963). Rather, it may be due to $\pi-\pi$ stacking that is known to occur when free-base protoporphyrin IX dimerizes. The experimentally observed absorbance changes at 464 nm were fitted to eq 14 using nonlinear regression, and a value of 2.1 μM was calculated for the equilibrium dissociation constant (K_d) of the dimer at 30 °C. (The derivation of this equation and the definition of the symbols are fully described in Materials and Methods.) The absorptivities of the monomer and dimer at 464 nm were 46 and 39 cm^{-1} mM^{-1}, respectively. Under the conditions typically used to measure the association between apocytochrome b_5 and Mn^{III} PPIX or Fe^{III} PPIX it was estimated that 50% of the Mn PPIX and 94% of the Fe PPIX was in the dimer form.

Determination of the Association Rate Constants for the Reactions between Apocytochrome b_5 and Its Ligands Mn PPIX and Heme. Our original intent in preparing the soluble form of Mn cytochrome b_5 was to characterize Mn cytochrome b_5 spectrally and to obtain crystals for X-ray diffraction studies. Although crystals of the native iron-containing protein were readily obtained, the manganese analog could not be crystallized. These results, together with the photoinstability noted when the resonance Raman spectrum was taken and the difficulties encountered in isolating Mn cytochrome b_5 free of the apoprotein, led us to suspect that the binding of Mn PPIX to apocytochrome b_5 was not tight. Studies were therefore undertaken to assess the extent of binding between Mn PPIX and apocytochrome b_5 under the conditions of our experiments with the reconstituted cytochrome P450 metabolizing system.

To follow the association of apocytochrome b_5 and its metalloporphyrin ligands spectrophotometrically, it was necessary to determine the wavelength maxima and the intensity of the spectral changes which were expected to occur during these reactions. The UV/vis spectra of the individual reaction components, Mn^{III} cytochrome b_5, Mn^{III} PPIX, ferric cytochrome b_5 and heme are presented in Figure 5. (Apocytochrome b_5 does not absorb in the range from 350 to 650 nm.) Spectral changes which occur during the association of apocytochrome b_5 with heme or Mn PPIX correspond to the difference spectra cytochrome b_5 minus heme and Mn^{III} cytochrome b_5 minus Mn^{III} PPIX, respectively. Typical difference spectra were calculated from the spectra of the individual components and are illustrated in Figure 6. Because the Mn^{III} and Fe^{III} PPIX spectra are concentration dependent these difference spectra vary with concentration. Using a split cell, difference spectra were also obtained experimentally. However, the experimentally obtained difference spectra differed significantly from the calculated spectra in the presence of heme. Subtraction of the experimental difference spectrum, obtained from the reaction of apocytochrome b_5 with heme in the split cell, from the calculated difference spectrum yielded the spectrum of heme. Therefore it was concluded that the lack of agreement between the calculated and experimental spectra is due to the loss of heme from the experimental solutions at pH 7.4, presumably as a result of adsorption of heme to surfaces when the contents of the split cell are mixed. Heme

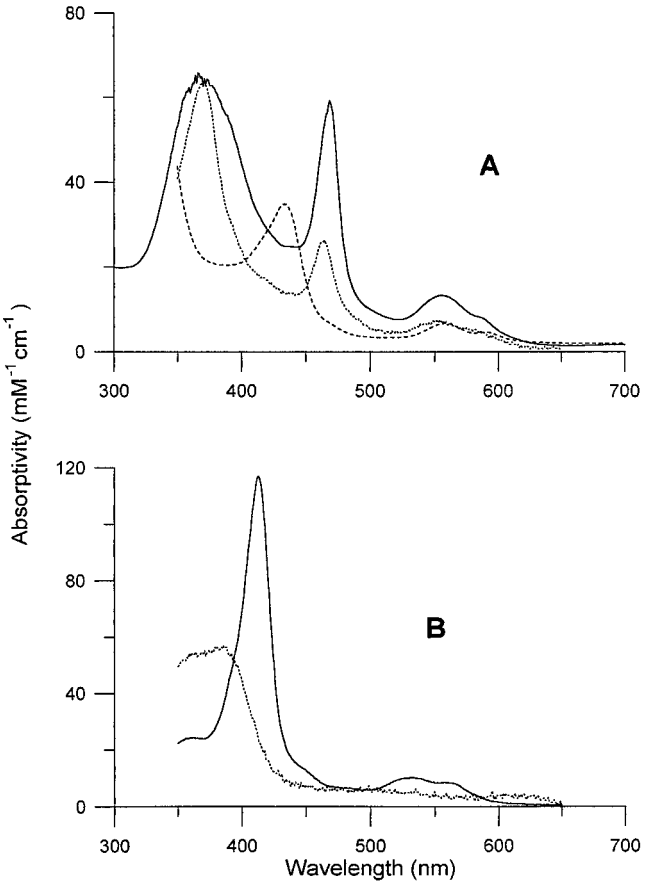

FIGURE 5: UV/vis absorption spectra (300−700 nm) of (A) oxidized Mn^{III} cytochrome b_5 (solid line), dithionite-reduced Mn^{II} cytochrome b_5 (dashed line), and Mn^{III} PPIX (dotted line). (B) Fe^{III} cytochrome b_5 (solid line) and Fe^{III} heme (dotted line).

was also lost from a phosphate buffer upon mixing. Although a linear increase in the absorbance at 385 nm was observed when aliquots of a heme solution were added to a 100 mM phosphate buffer at pH 7.4 to give final heme concentrations up to 8 μM, the solutions were not stable and an absorbance decrease was observed whenever the solutions were agitated. Similar problems with adsorption onto glassware has also been reported for Fe hematoferriprotoporphyrin IX (Brown & Hatzikonstantinou, 1979). The calculated rather than the experimental difference spectra were used as references. The wavelength maxima and absorptivity calculated from the difference spectra were ϵ_{414} = 92 mM^{-1} cm^{-1} for the association of heme and apocytochrome b_5 and at 470 nm ranged from 28 for the monomer to 41 mM^{-1} cm^{-1} (when 0.5 mM dimer reacts with 1 mM protein) for the association of Mn PPIX and apocytochrome b_5 (and depends on the Mn PPIX concentration). Association reactions were followed in the stopped-flow spectrophotometer at these wavelength maxima. Complete spectra were also taken during the association reactions which verified the expected spectral changes.

The rate of association of Mn PPIX or heme with apocytochrome b_5 was determined at fixed wavelength in the stopped-flow spectrophotometer under pseudo-first-order conditions. That is, at least a 5-fold excess of heme or Mn PPIX was present. A good fit of the absorption data could be obtained with a single exponential. Second-order rate constants were determined from these experiments by using the monomer concentrations calculated from the appropriate equilibrium dissociation constant. This approach assumes

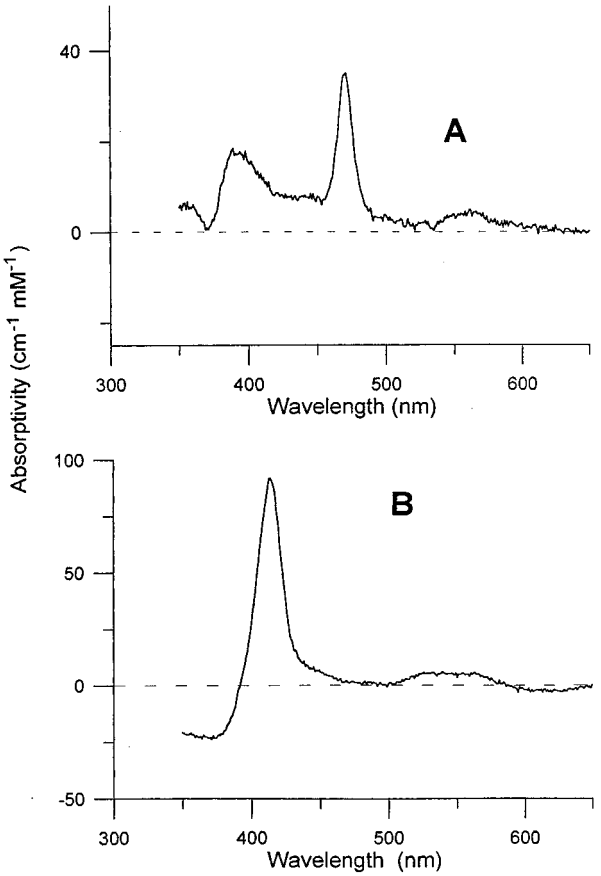

FIGURE 6: Calculated UV/vis difference spectra (A) Mn^{III} cytochrome b_5 minus Mn^{III} PPIX (B) Fe^{III} cytochrome b_5 minus Fe^{III} heme. These concentration-dependent spectra were calculated as described in Materials and Methods.

that the rate of dissociation of the dimer into monomer is rapid compared to the pseudo-first-order rate for the combination, of the heme or Mn PPIX with apocytochrome b_5. The validity of this assumption was confirmed by stopped-flow spectrophotometry with Mn PPIX. Dilution experiments demonstrated that the rate of dissociation of the dimer was too fast to be measured ($k \gg 100\ s^{-1}$). Our experiments also revealed a linear relationship between the pseudo-first-order rate constant for association of the calculated monomer of Mn^{III} PPIX concentration and apocytochrome b_5 over a $1-18\ \mu M$ Mn^{III} PPIX concentration range ($r^2 = 0.995$, $m = 13$). These results are consistent with our assumption that Mn PPIX is partially dimerized under our experimental conditions. The second-order rate constant for the association of Mn PPIX and apocytochrome b_5 at 20 °C was determined to be $3.3 \times 10^6\ M^{-1}\ s^{-1}$.

Because of its much greater tendency to form dimers and to adsorb to glassware, similar dilution experiments were not possible with Fe PPIX. However, when a 2 μM Fe PPIX solution was diluted with an equal amount of a 2 μM Mn PPIX solution in the stopped-flow spectrophotometer at 30 °C, spectral changes (a decrease in absorbance at 464 nm) were complete within 40 ms ($k_{\text{first order}} = 94\ s^{-1}$). The spectral changes were not explained by dilution of either Mn or Fe PPIX alone and were assumed to result from the formation of a mixed Mn PPIX−Fe PPIX dimer. This finding is consistent with a rapid conversion of dimeric Fe PPIX to the monomer. The association rate constant for experiments performed with Fe PPIX were, therefore, calculated by using the published equilibrium association constant (4.5) to estimate the Fe PPIX monomer concentrations (Brown et al., 1970). The association rate constant of Fe PPIX with apocytochrome b_5 was determined to be $4.5 \times 10^7\ M^{-1}\ s^{-1}$ at 20 °C. The rate constants were also determined with Mn PPIX at a number of other temperatures and are provided in Table 1. There was a modest increase in the rate of association with increasing temperature; an Arrhenius plot of the data between 20 and 37 °C gave an energy of activation, $\Delta G^{\ddagger}$, of 14 kcal/mol.

Table 1: Temperature Dependence of the Association Rate Constant and the Dissociation Rate and Equilibrium Constants of Mn Cytochrome b_5[a]

temp (°C)	k_f (s^{-1})[b]	A_f[b]	k_s (s^{-1})[b]	A_s[b]	% apo[c]	K_d (nM)[d]	k_{asn} ($\times 10^6\ M^{-1}\ s^{-1}$)[e]
20	0.27	0.0013	0.0121	0.0146	9	4	3.3
25	0.41	0.0017	0.0259	0.0160		ND[f]	
30	0.62	0.0028	0.0513	0.0217	13	7	6.9
37	2.18	0.0042	0.168	0.0227	17	14	12.4
45	6.35	0.0052	0.703	0.0211	21	32	21.8

[a] The dissociation of Mn cytochrome b_5 was followed in the stopped-flow spectrophotometer in the single wavelength mode at 414 nm. Initial concentrations in the observation cell of the stopped-flow spectrophotometer were 0.4 μM Mn cytochrome b_5 batch II and 1.5 μM heme. Absorbance changes at 414 nm were analyzed as biphasic exponentials by nonlinear regression. [b] k_f and k_s are the rate constants derived for the fast and slow phases of the dissociation of Mn cytochrome b_5, respectively; A_f and A_s are the respective absorbance changes of the indicated phase. [c] % apo is the fraction of the total amount of cytochrome b_5 present as apocytochrome b_5 at the beginning of the reaction. It was calculated from the equilibrium dissociation constant. [d] K_d is the calculated equilibrium constant for the dissociation of Mn cytochrome b_5 into Mn PPIX and apocytochrome b_5 and is given by the ratio of k_s/k_{asn}. [e] k_{asn} is the second order rate constant for association of apocytochrome b_5 and Mn PPIX. [f] ND, not determined.

Characterization of Mn Cytochrome b_5 Solutions and Determination of the Absorptivity of Mn Cytochrome b_5. Because of the loose binding between Mn PPIX and apocytochrome b_5, assessing the concentration of apocytochrome b_5 and holo Mn cytochrome b_5 in stock solutions for the purpose of determining the absorbtivity proved to be unexpectedly difficult. One indication of the poor binding of Mn PPIX to apocytochrome b_5 was the observation of two bands on a non-denaturing polyacrylamide gel of supposedly holo Mn cytochrome b_5 which had been isolated from a Sephadex G-25 gel column after treatment of apocytochrome b_5 with excess Mn PPIX. The faster running band was colored and was presumably due to the holoprotein. The second band was not colored and corresponded to apocytochrome b_5. The density of the apocytochrome b_5 band on the gel was not linear with the amount applied nor did apocytochrome b_5 have any distinct spectral features which would allow an accurate estimate of the amount present. The Mn cytochrome b_5 was finally isolated as two batches, Batch I and Batch II, which differed slightly in the amount of Mn PPIX that had been added.

The total net spectral changes expected to occur during the reaction of Mn cytochrome b_5 with heme were calculated by subtracting the spectra of the reactants (Mn cytochrome b_5 + heme) from the spectra of the products (cytochrome b_5 + Mn PPIX). Because spectral changes occur upon dimerization of the metalloporphyrins, this spectrum is concentration dependent. The wavelength maxima and absorptivity for this difference spectrum (Figure 7) were calculated to be $\epsilon_{414} = 88\ mM^{-1}\ cm^{-1}$ and $\epsilon_{470} = -33\ mM^{-1}\ cm^{-1}$ (range

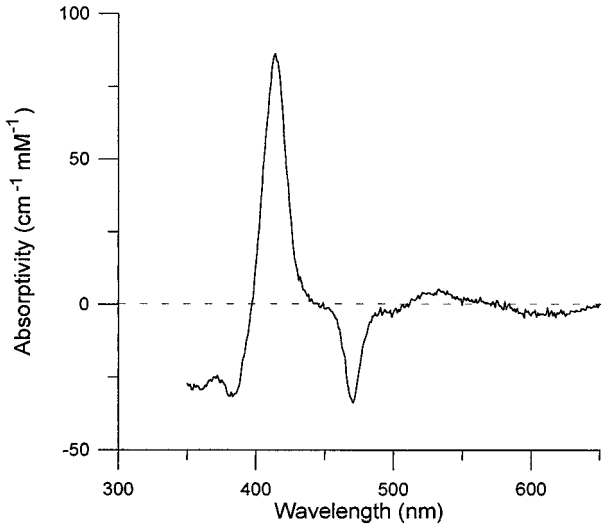

FIGURE 7: Calculated UV/vis difference spectrum of cytochrome b_5 plus 3.8 μM Mn PPIX minus heme (1.8 μM) minus Mn cytochrome b_5 at pH 7.9. These are the concentration-dependent spectral changes which are expected to occur as a result of the reaction of Mn cytochrome b_5 with heme.

-27 to -40 mM^{-1} cm^{-1}). A comparison of this calculated spectrum with those for the association reactions given above indicates that the absorbance change at 414 nm due to the dissociation of Mn cytochrome b_5 into Mn PPIX and apocytochrome b_5 is small ($\cong 10-15$ mM^{-1} cm^{-1}) compared to the absorbance change due to the reaction of apocytochrome b_5 with heme and, likewise, the reaction of apocytochrome does not contribute significantly to the absorbance decrease at 470 nm.

The concentration of apo and holo Mn cytochrome b_5 in solutions of diluted Batch I and II Mn cytochrome b_5 was determined by titration with known amounts of heme. (See Figure 8 for titration of Batch I.) A diluted stock solution of Batch I Mn cytochrome b_5 of less than 10 μM at 30 °C is expected to contain apocytochrome b_5 from two sources: (1) from the original stock solution and (2) from dissociation of Mn cytochrome b_5 into apocytochrome b_5 and Mn PPIX upon dilution. Figure 8 illustrates the three-phase titration of the unknown solution. In phase one (up to ~1 nmol of heme addition) little absorbance change at 470 nm is observed. However, control experiments demonstrate an increase in absorbance at 414 nm, indicating that the added heme is reacting with the apocytochrome b_5 present. In phase two, a marked absorbance decrease at 470 nm is observed which represents the displacement of MnPPIX from Mn cytochrome b_5 by heme. This phase was completed when ~4 nmol of heme were added. The total amount of apocytochrome b_5 present was determined from the amount of heme added at the intersection of the straight line formed by extrapolation of the phase II curve to zero absorbance change. The amount of apocytochrome b_5 present due to dissociation from Mn PPIX on dilution was calculated from the equilibrium dissociation constant of Mn cytochrome b_5 determined as described in the next section. The amount of apocytochrome b_5 present due to dissociation upon dilution was subtracted from the total amount of apocytochrome b_5 present to determine that present in the original concentrated Batch I preparation. In the third phase, the dissociated Mn PPIX reacts with the excess heme causing a further decrease at 470 nm. In this way, Batch II Mn cytochrome b_5 was found to contain nearly 100% holoprotein while Batch I Mn

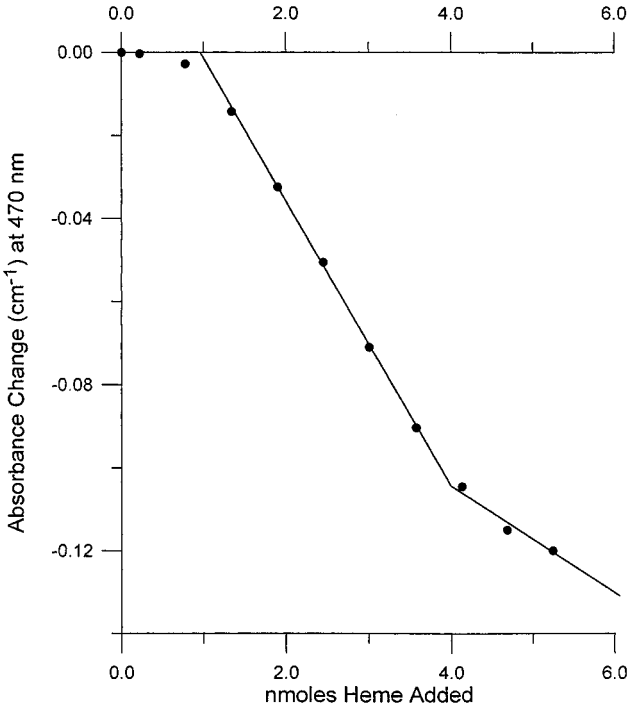

FIGURE 8: Absorbance changes occurring at 470 nm when Mn cytochrome b_5 (Batch I) in 100 mM potassium phosphate, pH 7.35, is titrated with a solution of heme in 50% ethanol and 0.2 mM sodium hydroxide as described in Materials and Methods. Heme was added to both the sample and reference cuvettes in the spectrophotometer, and the loss of Mn cytochrome b_5 was followed at 470 nm.

cytochrome b_5 contained 20% apocytochrome b_5. An $\epsilon_{469} = 57$ mM^{-1} cm^{-1} was estimated for Mn cytochrome b_5, assuming that Batch II Mn cytochrome b_5 contained 100% holoprotein. Previous values reported in the literature were 51 mM^{-1} cm^{-1} (Rogers & Strittmatter, 1974) and 38 mM^{-1} cm^{-1} (Morgan & Coon, 1984).

Determination of the Rate Constant for the Dissociation of Mn Cytochrome b_5 into Apocytochrome b_5 and Mn PPIX. Preliminary studies indicated that the association of apocytochrome b_5 with heme at a concentration of 1 μM was ~100 times faster than the dissociation of Mn PPIX from Mn cytochrome b_5. The reaction of heme with Mn cytochrome b_5 occurs in two steps. In the first rate-limiting step, Mn cytochrome b_5 dissociates into apocytochrome b_5 and Mn PPIX. This reaction was followed at 470 nm. In the second step, apocytochrome b_5 and Fe PPIX rapidly and essentially irreversibly react to form holocytochrome b_5. The association reaction can be observed at 414 nm. Because the second step is much faster, the increase in absorbance at 414 nm during the reaction of Mn cytochrome b_5 with heme will reflect the rate-limiting dissociation step.

(A) Rapid Scan Studies. Figure 9 illustrates the spectral changes which occur after rapidly mixing heme and Mn cytochrome b_5 solutions in the stopped-flow spectrophotometer. The first spectrum is approximately the sum of the free heme and the Mn cytochrome b_5 spectrum and hence has a large broad absorbance at about 370 nm. The rapid reaction of heme with the apocytochrome b_5 in the Mn cytochrome b_5 solution which can be observed when spectra are recorded in the fixed wavelength mode was completed before the second spectrum was recorded at 2 s. Therefore, the spectra shown only illustrate the simultaneous decrease in Mn cytochrome b_5 at 470 nm and increase in holo native

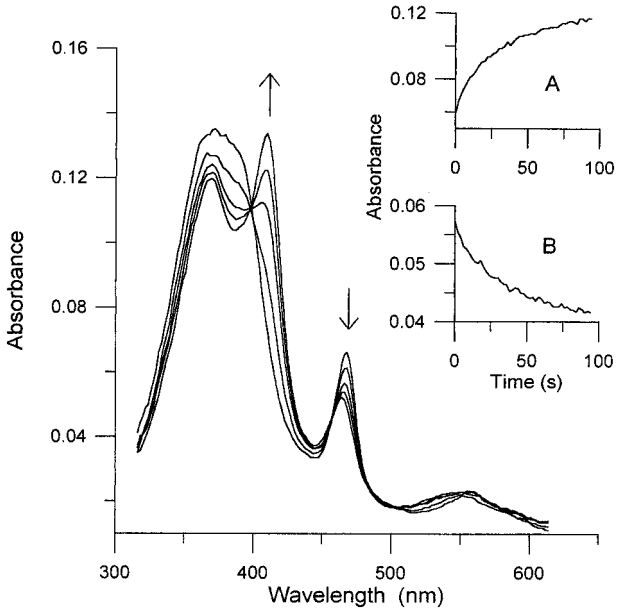

FIGURE 9: Spectral changes which occur following the rapid mixing of a solution of Mn cytochrome b_5 and heme are illustrated. Complete spectra were recorded every 2 s on a Hi-Tech SF-40 stopped-flow spectrophotometer. The insets show the absorbance changes at (A) 414 nm and (B) 470 nm as derived from the rapid scans. The experiments were performed as described in Materials and Methods.

cytochrome b_5 at 414 nm. Analysis of the spectral scan data at 470 and 414 nm shown in the inset of Figure 9 confirm that the rate of disappearance (B) of Mn cytochrome b_5 was the same as the rate of appearance (A) of cytochrome b_5 (at 25 °C, $k = 0.033$ s^{-1} at 470 and 0.035 s^{-1} at 414 nm, respectively).

(B) Fixed Wavelength Studies. In the studies of the dissociation of Mn cytochrome b_5 at fixed wavelength, a 3-fold excess of heme was used in order to minimize the recombination of Mn PPIX with apocytochrome b_5. Increasing the heme concentration further did not alter the data. Good fits of the dissociation data could only be obtained with a biphasic exponential. With Batch I Mn cytochrome b_5 the rate constant derived from the initial rapid phase at 414 nm was consistent with that expected for the association of apocytochrome b_5 with heme (data not shown). With Batch II Mn cytochrome b_5 the initial rapid phase accounted for a smaller percentage of the total absorbance change. It was assumed that only the slower of the two kinetic phases is due to the dissociation reaction. From this slower phase a dissociation rate constant of 0.0121 s^{-1} was calculated at 20 °C with both batches of Mn cytochrome b_5 (Table 1).

Dependence of the Equilibrium Dissociation Constant (K_d) and Rate Constant for the Dissociation of Mn PPIX from Mn Cytochrome b_5 on Temperature. Previous experiments, in our laboratory and in other laboratories, with the reconstituted cytochrome P450 system have been done at temperatures ranging from 20 to 37 °C. In order to have corresponding stability data for Mn cytochrome b_5, dissociation rate constants for Batch II Mn cytochrome b_5 were determined over a similar temperature range. These data (Table 1) demonstrate that the rate of the dissociation reaction increases rapidly with increasing temperature. An Arrhenius plot of the relation between the dissociation rate constant and temperature [ln(k) vs 1/T] was linear between 20 and 37 °C and gave an activation energy, $\Delta G^{\ddagger}$ of 27 kcal/mol.

Table 2: Influence of pH on the Rate Constant of the Dissociation of Mn Cytochrome b_5[a]

pH	k_f (s^{-1})[b]	A_f[b]	k_s (s^{-1})[b]	A_s[b]	% apo[c]
9.0	0.033	0.0024	0.0086	0.0134	15%
8.59	0.060	0.0028	0.0107	0.0147	16%
8.13	0.14	0.0033	0.0111	0.0189	14%
7.57	0.52	0.0042	0.0117	0.0251	14%
6.99	1.08	0.0053	0.0169	0.0218	19%
6.30	1.26	0.0076	0.0562	0.0140	34%

[a] Reactions were performed at 20 °C in a stopped-flow spectrophotometer with initial concentrations of 0.33 μM Mn cytochrome b_5 Batch I and 0.7 μM heme in the observation cell. Absorbance changes at 414 nm were analyzed as a biphasic exponential. [b] k_f and k_s are the rate constants derived for the fast and slow phases of the dissociation of Mn cytochrome b_5, respectively; A_f and A_s are the respective amplitudes of the absorbance changes. [c] % apo is the fraction of protein present as apocytochrome b_5 at the beginning of the reaction as calculated from the amplitudes of the absorbance changes in the fast and slow kinetic phases.

The equilibrium dissociation constants, K_d, for Mn cytochrome b_5, given in the next to the last column of Table 1, were calculated using the formula $K_d = k_s/k_{asn}$, where k_s is the slow rate constant for the dissociation of Mn cytochrome b_5 (Table 1) and k_{asn} is the second order rate constant for the association of Mn PPIX with apocytochrome b_5, determined in a separate set of experiments under identical experimental conditions. Note that the dissociation reaction rate constant increases more rapidly with temperature than the association reaction rate constant and as a result a greater equilibrium concentration of apocytochrome b_5 is formed at higher temperature. The fraction of Mn cytochrome b_5 which dissociates to apocytochrome b_5 and Mn PPIX under conditions which are typically used for the reconstituted cytochrome P450 system (Canova-Davis et al., 1985; Morgan & Coon, 1984) was calculated to range between 10−40%.

Effect of Ionic Strength and pH on the Dissociation of Mn Cytochrome b_5. The salt and pH dependence of the dissociation reaction was also examined. No effect on the rate of the dissociation reaction was seen with increasing potassium phosphate buffer concentrations from 50 to 500 mM. The pH dependence data are provided in Table 2. Below pH 7, there was an increase in the rate of the dissociation reaction which was consistent with the protonation of a group with a pK_a of 5.9, presumably the axial histidines. Ozols and Strittmatter (1964) saw a similar pH dependency for the dissociation of Fe^{III} hematoporphyrin IX (a dicarboxylic porphyrin with 2- and 4-hydroxyethyl groups) from apocytochrome b_5, whereas cytochrome b_5 itself was stable over the pH range from 6 to 9. The fraction of apocytochrome b_5 present at the beginning of the reaction was estimated from the derived amplitudes of the kinetic phases assuming that the fast kinetic phase is due to the reaction of apocytochrome b_5 with heme. The results are presented in Table 2. As expected from the dissociation data, the fraction of the protein present as apocytochrome b_5 increased at lower pH.

DISCUSSION

Our results demonstrate that the hexacoordinate Mn^{III} cytochrome b_5 is converted readily to pentacoordinate cytochrome b_5 by laser excitation at 476.5 nm. Other heme systems such as reduced alkaline cytochrome *c* peroxidase (CCP) which is postulated to have a bishistidyl coordination

have also been observed to undergo photodissociation of the axial ligand(s) under Soret excitation (Smulevich et al., 1989). In fact, Jongeward et al. (1988) have shown that the endogenous ligands in cytochrome *c* and cytochrome b_5 are subject to photolysis, but the ligands recombine in a few picoseconds so that the five-coordinate species is not observed in experiments that average over a longer time scale. A structural analysis of cytochrome b_5 has indicated that during photolysis the iron−histidine bond distance could be increased to over 3 Å (with bond breakage) by simply rotating the histidine α and β carbons 15−50 ° without exerting strain on the neighboring residues (Jongeward et al., 1988). Since the protein does not allow the photolyzed histidine to move far away, a fast recombination can occur between iron and the histidine via a simple rotation. The recombination of the photolyzed histidine to Mn^{III} can also be accomplished by a simple rotation of histidine α and β carbon bonds. When the photolyzed histidine recombines with Fe^{II} in native b_5, the d^6 system undergoes a transition from high-spin five-coordinate to a low-spin six-coordinate state. However, the d^4 system in Mn^{III} cytochrome b_5 remains high-spin, either five- or six-coordinate with a singly occupied d_z^2 orbital. This unfavorable configuration results in a smaller driving force for the recombination in Mn^{III} cytochrome b_5. The direct result of this small driving force could be either a slow recombination rate or high energy barrier.

Both the resonance Raman experiments and the studies of the binding of Mn PPIX to cytochrome b_5 indicate that cytochrome b_5 binds hemes more tightly by several orders of magnitude than Mn PPIX. Why is this? Studies of model compounds suggest an explanation (Hoard, 1975). Although Mn^{III} PPIX is the same size as heme and can readily fit into the heme cavity in cytochrome b_5, model compounds suggest that the Mn^{III}−imidazole bond of a bis(l-methylimidazole) tetraphenylporphyrin is rather long, 2.308 Å, and therefore weaker compared to the crystallographically determined homologous Fe^{III}−histidine bond of 2.04 Å in native cytochrome b_5 (Argos & Mathews, 1975; Mathews et al., 1972; W. R. Scheidt, personal communication). The long and therefore weak imidazole bond is attributed to the fact that Mn^{III} has a singly occupied d_z^2 orbital (Hoard, 1975). The ready dissociation of Mn^{III} PPIX from cytochrome b_5 is presumably due to the weak Mn^{III} axial histidine bonds. In hexacoordinate Mn^{III} cytochrome b_5 the Mn^{III} is expected to be in the plane of the porphyrin. The ferric ion is known from crystallographic studies to be in the plane of the heme in both ferric and ferrous native cytochrome b_5. However, in Mn^{III} cytochrome b_5 the metal ligand distance is expected to be increased by 0.3 Å on each side of the Mn PPIX. This should displace protein residues on either side of the Mn PPIX and enlarge the porphyrin binding pocket of cytochrome b_5, perhaps further destabilizing the protein−Mn PPIX binding. Without a crystal structure it is impossible to know in detail how the structure of cytochrome b_5 changes as a result of probably increasing the metal ligand distance by 0.3 Å. Presumably the volume of the protein will increase slightly and amino acid side chains in the vicinity of the axial ligands will rearrange to minimize the protein expansion. Nevertheless, the tertiary structures of Mn^{III} cytochrome b_5 is expected to be very similar, but not identical, to that of the native ferric protein. The crystal structure of Mn^{III} hemoglobin has revealed that its tertiary structure is similar to that of Fe^{III} hemoglobin. There are, however, a number of small but significant differences. The Mn^{III} PPIX substituted α chain is virtually unperturbed by the metal substitution. However, in the β chain the sixth ligand of the Mn^{III} PPIX, which is a water molecule in the native hemoglobin, has been lost. This has resulted in a contraction of the water ligand pocket in the β chain (Moffat et al., 1976). Mn^{III} cytochrome b_5 is the form of cytochrome b_5 that will exist under the aerobic conditions used in our reconstituted cytochrome P450 system. Mn^{II} cytochrome b_5 will be generated by reduction with cytochrome P450 reductase but will rapidly oxidize in the presence of oxygen. Recall that it is ferrous cytochrome b_5 which reduces cytochrome P450 (Morgan & Coon, 1984). Therefore, our conclusions are (1) that hexacoordinate Mn^{III} cytochrome b_5 is a good model for Fe^{II} cytochrome b_5, the form of the protein which reduces cytochrome P450 in the reconstituted system, and (2) that we and others were justified in using Mn^{III} cytochrome b_5 as a redox inactive form of ferrous cytochrome b_5 in our studies of the role of cytochrome b_5 in the cytochrome P450 reconstituted system (Canova-Davis et al., 1985; Morgan & Coon, 1984; Tamburini & Schenkman, 1987). The caveat here is that Mn cytochrome b_5 readily dissociates into the apoprotein and Mn PPIX.

Mn^{II} cytochrome b_5 is high-spin pentacoordinate according to our resonance Raman data. Model Mn^{II} porphyrin compounds indicate that the Mn^{II} atom which has the $d_{x^2-y^2}$ orbital occupied, in contrast to Mn^{III} where this orbital is empty, is displaced by ≅0.5 Å out of the plane of the heme toward the fifth ligand (Hoard, 1975; Kirner et al., 1977). In ferrous cytochrome b_5, the iron is in the plane of the porphyrin and the crystallographically determined ferrous−N_ϵ histidine bond length is 2.04 Å (Argos & Mathews, 1975). It is, therefore, expected that the protein on the side of the fifth ligand will be displaced away from the plane of the heme while the amino acid side chains near the empty sixth ligand position may rearrange and result in a contraction of the protein. Of course, without a crystal structure it is impossible to know the exact tertiary structure of Mn^{II} cytochrome b_5 and the above is only a hypothesis. The preceding consideration of the structure of Mn^{II} model porphyrins and their relationship to Mn^{II} cytochrome b_5 leads us to conclude that the structure of Mn^{II} cytochrome b_5 will be similar but not absolutely identical to native ferrous cytochrome b_5. The manganous form of cytochrome b_5 is capable of donating an electron while, as previously mentioned, Mn^{III} cytochrome b_5 is not capable of donating an electron.

Our studies have demonstrated that Mn PPIX dissociates from Mn cytochrome b_5 ($k = 1.2 \times 10^{-2}$ s^{-1} at 20 °C) about 1000 times faster than heme dissociates ($k = 1.67 \times 10^{-5}$ s^{-1}) from native cytochrome b_5 (Vergères et al., 1993). The K_d of Mn cytochrome b_5 at neutral pH and at temperatures varying from 20 to 37 °C was 4−14 nM while the K_d of heme from native cytochrome b_5 is estimated to be 0.0004 nM at 20 °C. Thus, under the conditions typically used in a reconstituted cytochrome P450 system, free Mn PPIX and apocytochrome b_5 will exist in solution. If the total protein concentration is 0.1 μM at 37 °C, it is estimated that 30% of the manganese substituted cytochrome b_5 may dissociate to form free Mn PPIX and apoprotein while at a Mn cytochrome b_5 of 1 μM about 90% of the protein will be present as Mn cytochrome b_5. It is therefore essential that

the stability of Mn cytochrome b_5 be confirmed under the conditions in which it will be used.

ACKNOWLEDGMENT

We are indebted to Dr. W. R. Scheidt for helpful discussions and for providing experimental results prior to publication.

REFERENCES

Argos, P., & Mathews, F. S. (1975) *J. Biol. Chem. 250*, 747−751.
Brown, S. B., & Hatzikonstantinou, H. (1979) *Biochim. Biophys. Acta 585*, 143−153.
Brown, S. B., Jones, P., & Lantzke I. R. (1969) *Nature 223*, 960−961.
Brown, S. B., Dean, T. C., & Jones, P. (1970) *Biochem. J. 117*, 733−739.
Canova-Davis, E., Chiang, J., & Waskell, L. (1985) *Biochem. Pharmacol. 34*, 1907−1912.
Cinti, D., & Ozols, J. (1975) *Biochim. Biophys. Acta 410*, 32−44.
Falzone, C., Mayer, M., Whiteman, E., Moore, C., & Lecomte, J. (1996) *Biochemistry 35*, 6519−6526.
Gruenke, L. D., Konopka, K., Cadieu, M., & Waskell, L. (1995) *J. Biol. Chem. 270*, 24707−24718.
Hoard, J. L. (1975) in *Porphyrins and Metalloporphyrins* (Smith, K., Ed.) pp 317−380, Elsevier Scientific Publishing Co., New York.
Jongeward, K., Magde, D., Taube, D., & Traylor, T. G. (1988) *J. Biol. Chem. 263*, 6027−6030.
Kalsbeck, W. A., Gosh, A., Pandey, R. K., Smith, K. M., & Bocian, D. F. (1995) *J. Am. Chem. Soc. 117*, 10959−69.
Kirner, J., Reed, C. A., & Scheidt, W. R. (1977) *J. Am. Chem. Soc. 99*, 2557−2563.
Loach, P. A., & Calvin, M. (1963) *Biochemistry 2*, 361−371.
Loehr, T. M., & Sanders-Loehr, J. (1993) *Methods Enzymol. 226*, 431−470.
Mathews, F. S., Levine, M., & Argos, P. (1972) *J. Mol. Biol. 64*, 449−464.
Mino, Y., Wariishi, H., Blackburn, N. J., Loehr, T. M., & Gold, M. H. (1988) *J. Biol. Chem. 263*, 7029−7036.
Moffat, K., Loe, R., & Hoffman, B. (1976) *J. Mol. Biol. 104*, 669−685.
Morgan, E. T., & Coon, M. J. (1984) *Drug Metab. Dispos. 12*, 358−364.
Oertling, W. A., Salehi, A., Chung, Y. C., Leroi, G. E., Chang, C. K., & Babcock, G. T. (1987) *J. Phys. Chem. 91*, 5887−5898.
Ozols, J., & Strittmatter, P. (1964) *J. Biol. Chem. 239*, 1018−1023.
Parthasarathi, N., & Spiro, T. G. (1987) *Inorg. Chem. 26*, 3792−3796.
Reid, L., & Mauk, A. G. (1982) *J. Am. Chem. Soc. 104*, 841−845.
Rogers, M., & Strittmatter, P. (1974) *J. Biol. Chem. 249*, 895−900.
Smulevich, G., Mauro, J. M., Fishel, L. A., English, A., Kraut, J., & Spiro, T. G. (1988) *Biochemistry 27*, 5477−5485.
Smulevich, G., Miller, M. A., Gosztola, D., & Spiro, T. G. (1989) *Biochemistry 28*, 9905−9908.
Spiro, T. G. (1983) in *Iron Porphyrins* (Lever, A. B. P., & Gray, H. B., Eds.) Part 2, Chapter 3, Addison-Wesley, Reading, MA.
Stavrov, S. S. (1993) *Biophys. J. 65*, 1942−1950.
Sun, J., Wilks, A., Ortiz de Montellano, P. R., & Loehr, T. M. (1993) *Biochemistry 32*, 14151−14157.
Tamburini, P., & Schenkman, J. (1987) *Proc. Natl. Acad. Sci. U.S.A. 84*, 11−15.
Teraoka, J., & Kitagawa, T. (1981) *J. Biol. Chem. 256*, 3969−3977.
Vergères, G., Wu, F. F., Chen, D. Y., & Waskell, L. (1993) *Arch. Biochem. Biophys. 305*, 231−241.
White, W. (1978) in *The Porphyrins* (Dolphin, D., Ed.) Vol. 5, Chapter 7, Academic Press, New York.
Yu, N. T. (1986) *Methods Enzymol. 130*, 350−409.

BI970407P